



Strong Nonreciprocal Mid-infrared Radiation at Small Angles Based on the Excitation of Guided Modes

Jun Wu,^{1,*} Yasong Sun,^{2,3} Biyuan Wu^{4,5} and Xiaohu Wu^{5,*}

Abstract

A strong nonreciprocal radiation effect, which is achieved by inserting a magneto-optical film between a one-dimensional metallic grating and a metallic reflector, is investigated. Strong nonreciprocal radiation is obtained at a wavelength around 15.5 μm when the incident angle is only 12° and the external magnetic field is 2 T. Such phenomenon is attributed to the critical coupling between the metal grating and guided mode resonances (GMRs) excited in the magneto-optical film. The physical mechanism is revealed by investigating the magnetic field distributions and verified through the coupled mode theory (CMT). In addition, the performances of thermal radiation for the designed emitter remain well in a wide range of geometric dimensions, which is friendly for fabrication. This work provides a new approach for designing nonreciprocal thermal emitters working at small angles. We believe that the designed structure can be employed to demonstrate Kirchhoff's law with nonreciprocal materials and enhance the efficiency of time-asymmetrical photovoltaics.

Keywords: Grating; Kirchhoff's law; Nonreciprocal radiation; Critical coupling.

Received: 07 January 2022; Revised: 07 February 2022; Accepted: 16 February 2022.

Article type: Research paper.

1. Introduction

It is well known that the directional spectral absorptivity of a structure is equal to the spectral emissivity in light of the traditional Kirchhoff's law,^[1-4] which results from the Lorentz reciprocity properties of Maxwell's equations.^[5] However, it is recently found that an emitter that consists of nonreciprocal materials, including magneto-optical materials^[6-9] and Weyl semimetals,^[10-12] can completely violate the fundamental Kirchhoff's law. For the materials mentioned above, the permittivity tensors are asymmetric, thus breaking the Lorentz reciprocity.^[13,14] The generalized Kirchhoff's laws, validating not only nonreciprocal devices but also reciprocal devices, have already been proposed in recent years.^[15-17]

When the emissivity is different from the absorbance, it is usually referred to as nonreciprocal radiation. Zhu *et al.* proposed a grating scheme made of magneto-optical material (InAs), where strong nonreciprocal radiation is achieved around 15.96 μm with a magnetic field of 3 T.^[6] Later, Zhao *et al.* proposed a novel structure consisting of an InAs film inserted between a silicon carbide (SiC) grating and an aluminum (Al) substrate, where near-complete nonreciprocal radiation is achieved with a magnetic field of only 0.3 T.^[7] Though the magnetic field used is small enough, the operating wavelength is as long as about 25 μm . Various materials and schemes have been designed to achieve nonreciprocal radiation as strongly as possible. However, Kirchhoff's law with nonreciprocal material has not yet been experimentally demonstrated until now.

Green has demonstrated that the nonreciprocal radiation is promising to overcome the Shockley-Queisser (SQ) limit of photovoltaics.^[18] Thus, novel energy-harvesting devices with more advanced features can be achieved by the hybridization of the traditional photovoltaic device with nonreciprocal materials. To improve the efficiency of photovoltaics, the angle between the light of the sun and the normal of the solar cells should be as small as possible. Thus, achieving strong nonreciprocal radiation with an incident angle as small as possible is highly desirable. In addition, the difference in absorption and emission is promising to be used in radiative

¹ College of Electrical Engineering, Anhui Polytechnic University, Wuhu, 241000, China.

² Basic Research Center, School of Power and Energy, Northwestern Polytechnical University, Xi'an 710064, Shaanxi, China.

³ Center of Computational Physics and Energy Science, Yangtze River Delta Research Institute of NPU, Northwestern Polytechnical University, Taicang 215400, Jiangsu, China.

⁴ School of Automation and Information Engineering, Xi'an University of Technology, Shaanxi, Xi'an 710048, China.

⁵ Shandong Institute of Advanced Technology, Jinan 250100, China

*E-mail: mailswj2011@163.com (J. Wu); xiaohu.wu@iat.cn (X. Wu)

cooling to improve the cooling power.^[19]

Besides, the energy of radiation at the direction of θ (θ denotes the angle between the normal interface and the direction of radiation) is proportional to $\cos \theta$. Such a phenomenon results from Lambert's law. Thus, the thermal emission signal is larger at smaller angles. In general, to demonstrate Kirchhoff's law with nonreciprocal materials, the thermal emissivity should be accurately measured. Therefore, realizing strong nonreciprocal radiation at smaller angles will strengthen the thermal emission signal, which is an advantage for measuring the emissivity in the experiment.^[20-22]

Whether from the perspective of practical application or experimentally verification, it is of great importance to achieve strong nonreciprocal radiation with the incident angle as small as possible. Until now, the majority of the proposed nonreciprocal emitters could achieve strong nonreciprocal radiation for incident angles as larger as 60° .^[6-8] Wu *et al.* utilized a magneto-optical material-dielectric multilayer structure to achieve strong nonreciprocal radiation at 30° .^[23] Their results indicated that the nonreciprocity can reach 0.87 at the incident angle of 30° , which results from the excitation of Tamm plasmon polaritons at the interface of the magnetophotonic crystal and the metal mirror. However, the angle is not small enough and should be further modified. Therefore, it is urgent to figure out an effective approach to realize enhanced nonreciprocal radiation for angles smaller than 30° .

Here, the enhanced nonreciprocal radiation effect with a novel structure which consists of a top metallic grating, a middle InAs film, and a bottom metallic mirror, is proposed and studied. The emitter exhibits near-complete nonreciprocal radiation at a wavelength of around $15.5 \mu\text{m}$ for a magnetic field of 2 T and an incident angle of 12° . The distribution of the normalized magnetic field magnitude as well as the CMT, are used to reveal the physical origin. Besides, the influence of the geometric dimensions on the radiation is studied in detail. The structure proposed in this work outperforms the structure proposed in Ref.^[23]. Thus, it can be employed to demonstrate the generalized Kirchhoff's law. This work provides a new approach for designing nonreciprocal thermal emitters working at small angles.

2. Design and method

The designed structure is illustrated in Fig. 1, where the direction of the magnetic field is along the y -axis. The proposed emitter is composed of three layers: a top aluminum (Al) grating, a middle InAs film, and a bottom Al mirror. The emitter can be considered to be supported by a dielectric substrate. The top Al grating is described by its period d , grating ridge width w , and grating thickness h . The thickness of the InAs spacer is h_s . The permittivity of the material Al is calculated according to the Drude model (1):

$$\alpha(\theta, \lambda) = 1 - R(\theta, \lambda) - T(\theta, \lambda), \quad \alpha(-\theta, \lambda) = 1 - R(-\theta, \lambda) - T(-\theta, \lambda),$$

$$\epsilon_{Al} = \epsilon_\infty - \frac{\omega_p^2}{\omega^2 + i\omega\Gamma}, \quad (1)$$

where $\epsilon_\infty = 1$, $\Gamma = 1.24 \times 10^{14}$ rad/s and $\omega_p = 2.24 \times 10^{16}$ rad/s.^[24] The thickness of the metallic reflector is fixed at $0.2 \mu\text{m}$, which is optically thick and will prevent light from passing through the device.

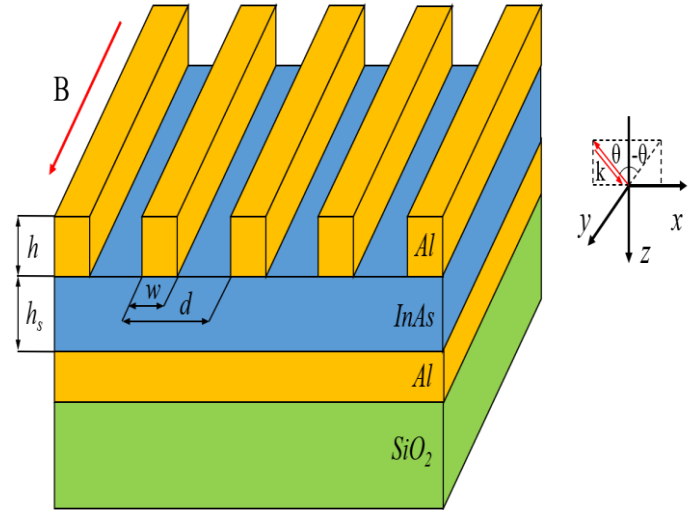


Fig. 1 Schematic of the designed structure for near-perfect nonreciprocal radiation.

In this work, the case of TM (transverse magnetic) polarized light is considered. Now, the dielectric constant tensor of InAs is described as^[6,25]:

$$\epsilon = \begin{bmatrix} \epsilon_{xx} & 0 & \epsilon_{xz} \\ 0 & \epsilon_{yy} & 0 \\ \epsilon_{zx} & 0 & \epsilon_{zz} \end{bmatrix}, \quad (2)$$

where,

$$\epsilon_{xx} = \epsilon_{zz} = \epsilon_\infty - \frac{\omega_p^2(\omega + i\Gamma)}{\omega[(\omega + i\Gamma)^2 - \omega_c^2]}, \quad (3)$$

$$\epsilon_{xz} = -\epsilon_{zx} = i \frac{\omega_p^2 \omega_c}{\omega[(\omega + i\Gamma)^2 - \omega_c^2]}, \quad (4)$$

$$\epsilon_{yy} = \epsilon_\infty - \frac{\omega_p^2}{\omega(\omega + i\Gamma)}. \quad (5)$$

The definite definitions and the parameter values employed in Eqs. (2)-(5) should be referred to Ref.^[7] The dielectric constant of the InAs does not vary with the temperature since the temperature employed in our device is above 300 K.^[6] The dependence of cyclotron frequency on the magnetic field is described by: $\omega_c = eB/m^*$, where m^* is the effective electron mass. Therefore, the magnetic field can influence the permittivity tensor by influencing the cyclotron frequency ω_c .

During the simulation, the directional spectral absorptivity and directional spectral emissivity of the devices are calculated according to^[15]

$$e(\theta, \lambda) = 1 - R(-\theta, \lambda) - T(\theta, \lambda), e(-\theta, \lambda) = 1 - R(\theta, \lambda) - T(-\theta, \lambda) \quad (6)$$

where R and T denote the corresponding reflectivity and transmissivity, respectively, and θ and $-\theta$ denote the incident angle, which is calculated by the mean of the rigorous coupled-wave analysis (RCWA).^[26-28] It is noted that Eq. (6) is not explicitly presented in this form in Ref.^[15], the reason is that the polarization conversion between the transverse magnetic wave and the transverse electric wave is not considered here. The difference between emission and absorption measures the nonreciprocal radiation. Therefore, the nonreciprocal radiation becomes stronger with the increase of the difference. The RCWA has often been employed to solve Maxwell's equations with grating-based devices, where the electromagnetic fields are expanded to the Fourier series. Detailed information about this method can be found in a previously published article.^[26]

By selecting initial geometric dimensions and employing the simulated annealing (SA) algorithm, we can obtain the final parameters. The objective function is:

$$\phi(d, w, h, h_s) = -A_{max} \quad (7)$$

where, $A_{max} = \max(A_{B=0 T}(\lambda))$, $A_{B=0 T}(\lambda)$ is the absorption spectra for $B = 0$ T. The process of optimization is to find appropriate geometric dimensions in order that $\phi(d, w, h, h_s)$ is minimum.

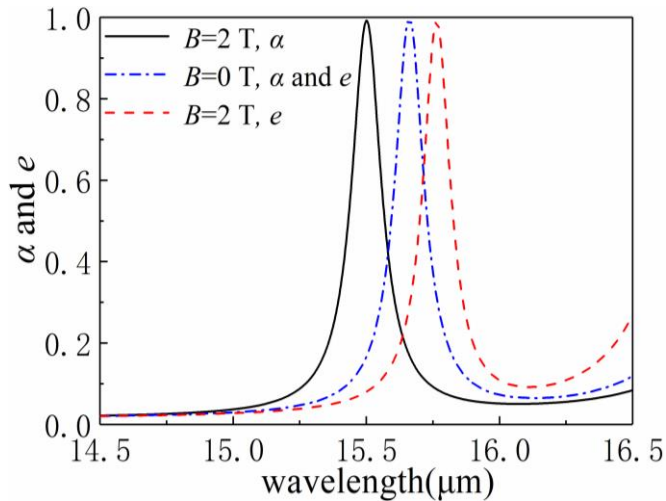


Fig. 2 The absorptivity (α) and emissivity (e) spectrum for $\theta = 12^\circ$ with $B = 0$ and $B = 2$ T.

3. Results and discussion

The structure parameters of the emitter are: $d = 7.5 \mu\text{m}$, $h = 0.55 \mu\text{m}$, $w = 3.0 \mu\text{m}$, and $h_s = 2.15 \mu\text{m}$. Then, we simulate the absorptivity spectra and the emissivity spectra for $\theta = 12^\circ$ with $B = 0$ T and 2 T, respectively, shown in Fig. 2. Obviously, the absorptivity and emissivity spectra are the same for $B = 0$. In contrast, with the magnetic field increasing from $B = 0$ to $B = 2$ T, the absorptivity spectra shift to a smaller wavelength while the emissivity spectra shift to a larger wavelength, which presents a violation of the typical Kirchhoff's law. Moreover,

the nonreciprocity, namely the difference between the peaks of emission and absorption, is nearly 0.911 at the wavelength of $15.5 \mu\text{m}$, which shows near-complete nonreciprocal radiation. Compared to Ref.^[23], the proposed structure in this work can reach stronger nonreciprocal radiation at smaller angles. Thus, this structure can be employed to demonstrate the generalized Kirchhoff's law and improve the efficiency of photovoltaics.

To reveal the physical origin of this effect, we show the calculated normalized magnetic field distribution at $\lambda = 15.5 \mu\text{m}$ of $\theta = 12^\circ$ and $\theta = -12^\circ$ in Figs. 3(a) and 3(b), respectively. Here, the magnetic field magnitude is normalized to the incident magnetic field. Clearly, when $\theta = 12^\circ$, the magnitude H_y is intensively enhanced and strongly concentrated in the InAs film, which exhibits the characteristic of GMRs.^[29,30] The maximum magnetic field enhancement can be larger than 20. As a result, the critical coupling is achieved due to the excitation of GMRs, which leads to perfect absorption in the devices. By contrast, the enhancement of the magnetic field in the middle InAs spacer for $\theta = -12^\circ$ is much weaker than that for $\theta = 12^\circ$, which leads to a tiny absorption. The maximum magnetic field enhancement, in this case, is smaller than 7.

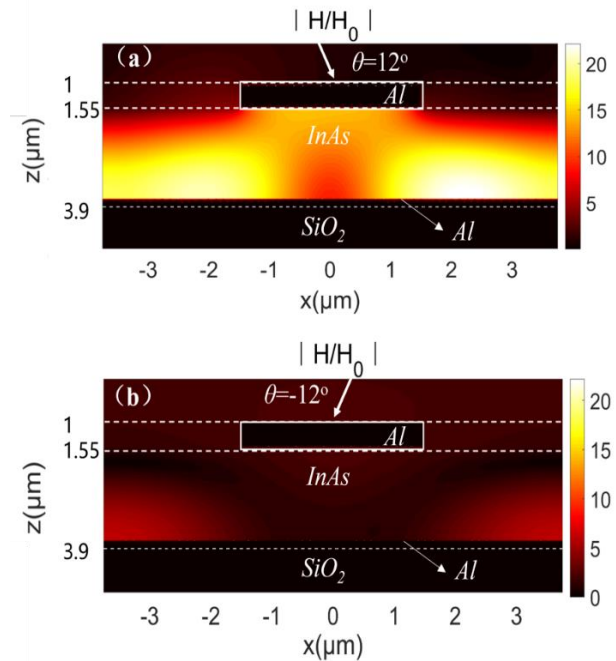


Fig. 3 The distribution of $|H_y/H_0|$ for (a) $\theta = 12^\circ$ and (b) $\theta = -12^\circ$.

To further confirm the critical coupling, the CMT is employed, as presented in Fig. 4. The reflection coefficient can be described as^[31,32]

$$r = \frac{i(\omega - \omega_0) + \delta - \gamma}{i(\omega - \omega_0) + \delta + \gamma} \quad (8)$$

where ω_0 is the angular frequency at resonance, δ and γ are the external leakage rate and the intrinsic loss rate, respectively.

The absorptivity can be expressed in^[31,32]

$$\alpha = 1 - |r|^2 = \frac{4\delta\gamma}{(\omega - \omega_0)^2 + (\delta + \gamma)^2} \quad (9)$$

From Eq. (9), it is found that the critical coupling condition is achieved when $\delta = \gamma$ and $\omega = \omega_0$. At this point, the energy of the incident plane wave will be completely absorbed by the device. γ and δ can be achieved by fitting the simulated and theoretical results. Only the absorptivity spectrum is used to verify the critical coupling. The fitting values are $\delta = \gamma = 0.28$ THz at $\omega_0 = 1.216 \times 10^{14}$ rad/s (15.5 μm). The excellent fitting in the neighborhood of the resonant wavelength validates the underlying mechanism.

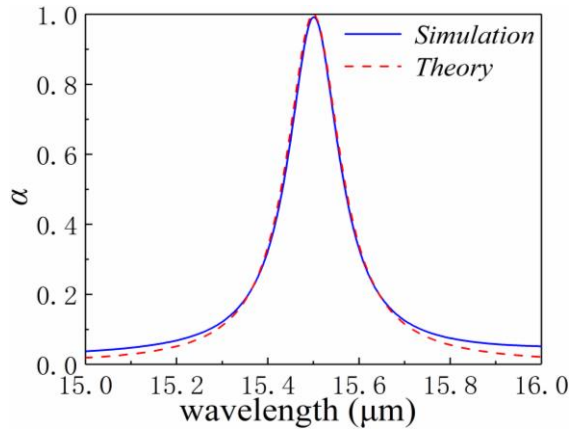


Fig. 4 Simulated and theoretical absorption spectra for the incident angle of 12° under the magnetic field of 2 T.

For practical application, the designed emitter should be fabricated at a low cost. Under this circumstance, the effect of the geometric parameters on the absorptivity and emissivity spectra are calculated and shown in Fig. 5. From Fig. 5(a), we found that both the absorptivity and emissivity spectra show a redshift when the period d increases from 7.4 μm to 7.6 μm . In addition, perfect absorptivity and emissivity can remain. When the width of the strips w increases from 2.9 μm to 3.1 μm , the absorptivity and emissivity spectra exhibit a redshift, with both peak absorptivity and emissivity remaining stable, as clearly shown in Fig. 5(b). Fig. 5(c) denotes the absorptivity and emissivity spectra with two different grating thicknesses h . It can be seen that the absorptivity and emissivity spectra are not sensitive to h as the peaks of the absorptivity and the emissivity are almost unchanged. Fig. 5(d) illustrates the absorptivity and emissivity spectra when h_s increases from 2.1 μm to 2.2 μm . Clearly, both peaks exhibit redshifts with the increasing of h_s . Besides, a relatively stable absorptivity and emissivity above 97.7% can be obtained. Generally, the near-complete nonreciprocal radiation performance, as well as perfect absorptivity and emissivity, remain excellent in a large geometric dimensions range, which should be an advantage for real manufacture. In addition, the sensitivity of the nonreciprocal radiation on the structure dimensions could also be used to change the operating wavelength of the nonreciprocal radiation.

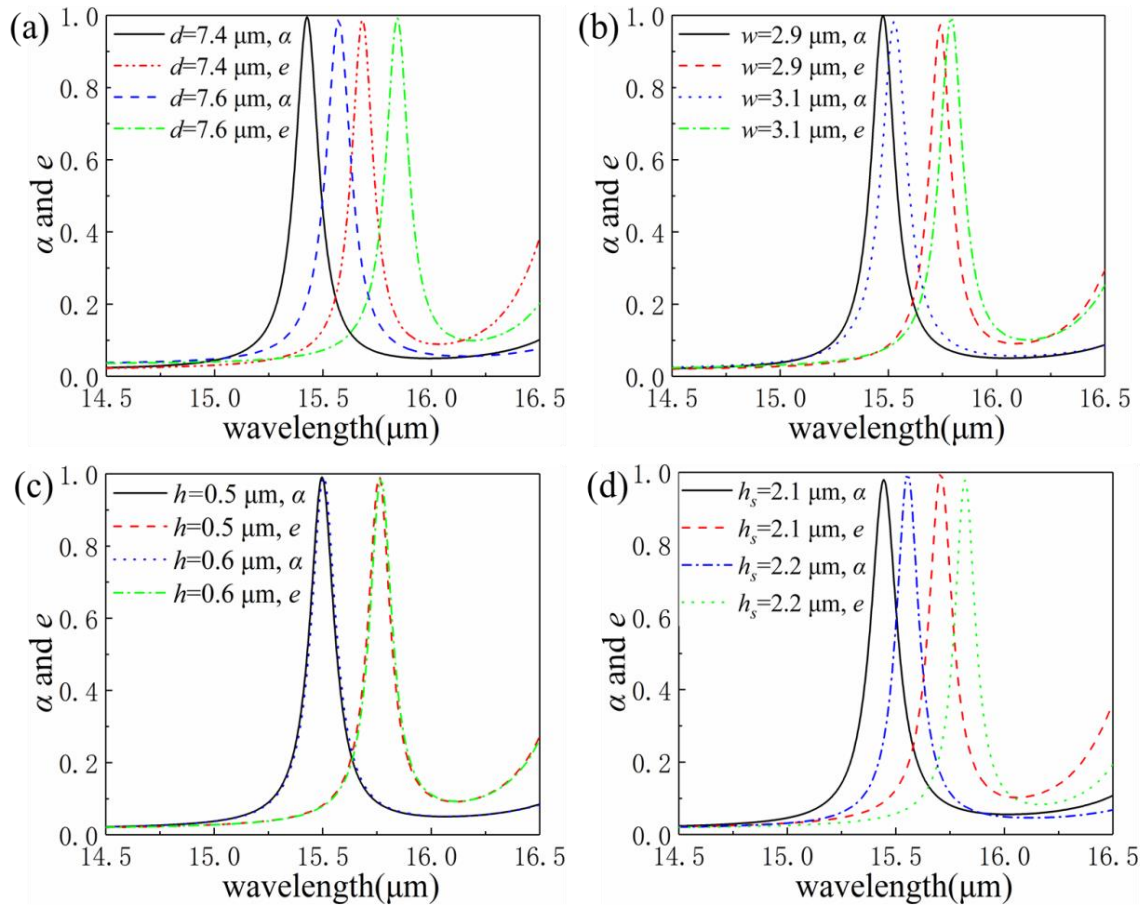


Fig. 5 α and e versus the change of: (a) d , (b) w , (c) h , and (d) h_s .

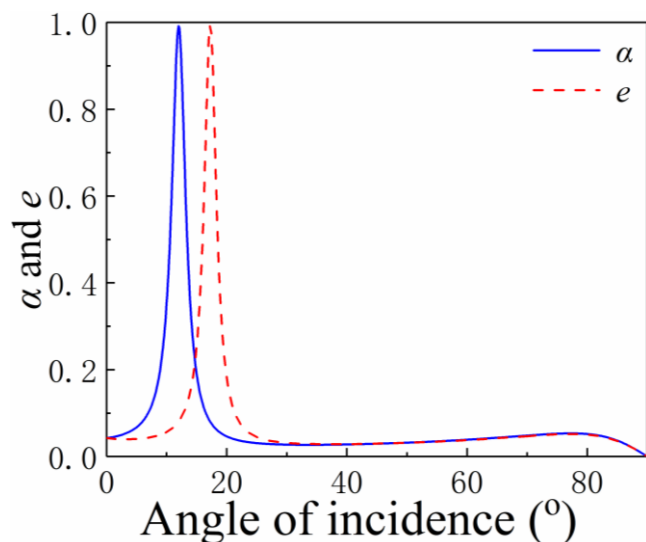


Fig. 6 α and e as a function of the incident angle at $\lambda = 15.5 \mu\text{m}$ with $B = 2 \text{ T}$.

The absorptivity and emissivity spectra versus the change of the angle of incidence are plotted in Fig. 6. The maximum absorptivity and emissivity are located at 12° and 17.3° , respectively. Both peaks are very sharp and their values of them can reach 0.99. The absorptivity and emissivity spectra almost overlap when the incident angle is more than 25° . In addition, they are smaller than 0.06 when the incident angle is more than 25° . Clearly, the angular widths for the absorptivity and emissivity spectra are about 2.9° and 2.6° , respectively. Since the inverse relation of the coherence length to its angular width,^[33] the proposed structure exhibits excellent spatial coherence. The such phenomenon indicates that the proposed structure in this paper could act as a highly directional thermal emitter and performs similarly to an antenna.^[33-35]

Up to now, most of the designed nonreciprocal thermal emitters are operated under an incident angle as large as 60° since strong nonreciprocity is more easily achieved at a larger incident angle.^[6-8,36] Only recently, some research had been proposed to realize strong nonreciprocal radiation around 30° .^[23,37-40] However, these structures usually suffer from low nonreciprocity (less than 0.9),^[23] large size^[37,38] along with not small enough incident angle (larger than 25°).^[23,37-40] Therefore, the key innovation of this work is that a nonreciprocity as large as 0.911 is achieved at an incident angle of only 12° along with a simple structure, which is superior to the schemes proposed in previous works.

4. Conclusions

In conclusion, the enhanced nonreciprocal radiation effect with a novel structure which consists of a metallic grating, an InAs spacer, and a bottom metallic mirror, is studied. Strong nonreciprocity, as larger as 0.911, can be achieved with a magnetic field of 2 T under an incident angle of 12° . The physical origin is disclosed by studying the normalized magnetic field magnitude distributions. Besides, the

mechanism is further confirmed by the CMT. In addition, the performances of the nonreciprocal radiation are maintained excellent within a wide varying range of geometric parameters, which should be beneficial for real manufacture. The proposed structure will prompt the development of nonreciprocal emitters and time-asymmetrical photovoltaics.

Acknowledgments

The authors acknowledge the support of the National Natural Science Foundation of China (Grant Nos. 61405217, 52106099), the Zhejiang Provincial Natural Science Foundation (Grant No. LY20F050001), the Anhui Provincial Natural Science Foundation (Grant No. 2108085MF231), the Anhui Polytechnic University Research Startup Foundation (Grant No. 2020YQQ042), the Pre-research Project of National Natural Science Foundation of Anhui Polytechnic University (Grant No. Xjky02202003), the Natural Science Foundation of Shandong Province (Grant No. ZR2020LLZ004).

Conflict of interest

There are no conflicts to declare.

Supporting information

Not applicable.

References

- [1] G. Kirchhoff, *Annalen Der Physik Und Chemie*, 1978, **185**, 275-301, doi: 10.1002/andp.18601850205.
- [2] M. Planck, The theory of heat radiation, *Forgotten Books*, 2010, Corpus ID: 119731114.
- [3] J. R. Howell, M. P. Menguc, R. Siegel, Thermal Radiation Heat Transfer, *CRC Press*, 2015, 1040, doi: 10.1201/9780429327308.
- [4] Z. M. Zhang, Nano/Microscale Heat Transfer, *McGraw-Hill*, 2007, doi: 10.1007/978-3-030-45039-7.
- [5] L. Landau, E. M. Lifshitz, J. Sykes, J. Bell, E. Dill, Electrodynamics of continuous media, *American Institute of Physics*, 1961, **14**, doi: 10.1063/1.3057154.
- [6] L. Zhu, S. H. Fan, *Physical Review B*, 2014, **90**, 220301, doi: 10.1103/PhysRevB.90.220301
- [7] B. Zhao, Y. Shi, J. Wang, Z. Zhao, N. Zhao, S. Fan, *Optics Letters*, 2019, **44**, 4203, doi: 10.1364/ol.44.004203.
- [8] X. Wu, *ES Energy & Environment*, 2021, **12**, 46-51, doi: 10.30919/eseec8c1047.
- [9] X. H. Wu, Z. X. Chen, F. Wu, *ES Energy Environment*, 2021, **13**, 8-12, doi: 10.30919/eseec8c442.
- [10] B. Zhao, C. Guo, C. A. C. Garcia, P. Narang, S. Fan, *Nano Letters*, 2020, **20**, 1923-1927, doi: 10.1021/acs.nanolett.9b05179.
- [11] Y. Tsurimaki, X. Qian, S. Pajovic, F. Han, M. Li, G. Chen, *Physical Review B*, 2020, **101**, 165426, doi:

- 10.1103/physrevb.101.165426.
- [12] S. Pajovic, Y. Tsurimaki, X. Qian, G. Chen, *Physical Review B*, 2020, **102**, 165417, doi: 10.1103/physrevb.102.165417.
- [13] S. Pajovic, Y. Tsurimaki, X. Qian, S. V. Boriskina, *Optical Materials Express*, 2021, **11**, 3125, doi: 10.1364/ome.435823.
- [14] Y. Li, W. Li, T. Han, X. Zheng, J. Li, B. Li, S. Fan, C.-W. Qiu, *Nature Reviews Materials*, 2021, **6**, 488-507, doi: 10.1038/s41578-021-00283-2.
- [15] Z. M. Zhang, X. H. Wu, C. J. Fu, *Journal of Quantitative Spectroscopy & Radiative Transfer*, 2020, **245**, 106904, doi: 10.1016/j.jqsrt.2020.106904.
- [16] D. A. B. Miller, L. Zhu, S. Fan, *Proceedings of the National Academy of Sciences*, 2017, **114**, 4336-4341, doi: 10.1073/pnas.1701606114.
- [17] C. Khandekar, F. Khosravi, Z. Li, Z. Jacob, *New Journal of Physics*, 2020, **22**, 123005, doi: 10.1088/1367-2630/abc988.
- [18] M. A. Green, *Nano Letters*, 2012, **12**, 5985-5988, doi: 10.1021/nl3034784.
- [19] R. Y. M. Wong, C. Y. Tso, C. Y. H. Chao, B. Huang, M. P. Wan, *Solar Energy Materials and Solar Cells*, 2018, **186**, 330-339, doi: 10.1016/j.solmat.2018.07.002.
- [20] Y. Xiao, A. Shahsafi, C. Wan, P. J. Roney, G. Joe, Z. Yu, J. Salman, M. A. Kats, *Physical Review Applied*, 2019, **11**, 014026, doi: 10.1103/physrevapplied.11.014026.
- [21] K. Zhang, K. Yu, Y. Liu, Y. Zhao, *International Journal of Heat and Mass Transfer*, 2017, **114**, 1037-1044, doi: 10.1016/j.ijheatmasstransfer.2017.06.133.
- [22] L. P. Wang, Z. M. Zhang, *Journal of Heat Transfer*, 2013, **135**, 091505, doi: 10.1115/1.4024469.
- [23] X. H. Wu, R. Y. Liu, H. Y. Yu, B. Y. Wu, *Journal of Quantitative Spectroscopy and Radiative Transfer*, 2021, **272**, 107794, doi: 10.1016/j.jqsrt.2021.107794.
- [24] M. A. Ordal, R. J. Bell, R. W. Alexander, L. L. Long, M. R. Querry, *Applied Optics*, 1985, **24**, 4493, doi: 10.1364/ao.24.004493.
- [25] K. Seeger, *Semiconductor Physics: An Introduction Springer Science & Business Media*, 2004.
- [26] X. Wu, C. Fu, Z. M. Zhang, *ES Energy & Environment*, 2020, **8**, 5-14, doi: 10.30919/eseec8c396.
- [27] L. Li, *Journal of the Optical Society of America A*, 1996, **13**, 1870-1876, doi: 10.1364/JOSAA.13.001870.
- [28] L. Li, *Journal of Optics A: Pure and Applied Optics*, 2003, **5**, 345-355, doi: 10.1088/1464-4258/5/4/307.
- [29] W. Liu, Y. Li, H. Jiang, Z. Lai, H. Chen, *Optics Letters*, 2013, **38**, 163, doi: 10.1364/ol.38.000163.
- [30] F. Wu, J. Wu, Z. Guo, H. Jiang, Y. Sun, Y. Li, J. Ren, H. Chen, *Physical Review Applied*, 2019, **12**, 014028, doi: 10.1103/physrevapplied.12.014028.
- [31] J. R. Piper, S. Fan, *ACS Photonics*, 2014, **1**, 347-353, doi: 10.1021/ph400090p.
- [32] X. Wang, J. Duan, W. Chen, C. Zhou, T. Liu, S. Xiao, *Physical Review B*, 2020, **102**, 155432, doi: 10.1103/physrevb.102.155432.
- [33] Y. Gong, X. Liu, K. Li, J. Huang, J. J. Martinez, D. Rees-Whippey, S. Carver, L. Wang, W. Zhang, T. Duan, N. Copner, *Physical Review B*, 2013, **87**, 205121, doi: 10.1103/physrevb.87.205121.
- [34] M. Laroche, R. Carminati, J. J. Greffet, *Physical Review Letters*, 2006, **96**, 123903, doi: 10.1103/physrevlett.96.123903.
- [35] B. J. Lee, Z. M. Zhang, *Journal of Heat Transfer*, 2007, **129**, 17-26, doi: 10.1115/1.2401194.
- [36] J. Wu, Z. Wang, H. Zhai, Z. Shi, X. Wu, F. Wu, *Optical Materials Express*, 2021, **11**, 4058, doi: 10.1364/ome.444308.
- [37] X. H. Wu, H. Y. Yu, F. Wu, B. Y. Wu, *AIP Advances*, 2021, **11**, 075106, doi: 10.1063/5.0055418.
- [38] J. Wu, F. Wu, T. Zhao, H. Zhai, X. Wu, *Engineered Science*, 2021, **18**, 141-147, doi: 10.30919/es8d575.
- [39] J. Wu, F. Wu, X. H. Wu, *Optical Materials*, 2021, **120**, 111476, doi: 10.1016/j.optmat.2021.111476.
- [40] J. Wu, F. Wu, T. C. Zhao, X. H. Wu, *International Journal of Thermal Sciences*, 2022, **172**, 107316, doi: 10.1016/j.ijthermalsci.2021.107316.

Author information



Jun Wu is an associate research fellow of Anhui Polytechnic University, working in nanophotonics, diffractive optics and metasurface. He received Ph.D degree from Shanghai Institute of Optics and Fine Mechanics in 2013. He was once an assistant research fellow from 2013 to 2015 and an associate research fellow from 2015 to 2018, working in Shanghai Institute of Optics and Fine Mechanics. He has published 70 journal and conference papers.



Xiaohu Wu received his B.S. degree in engineering mechanics from China University of Mining and Technology (Beijing) and Ph. D. degree from Peking University under the guidance of Prof. Ceji Fu. He was a visiting student at Georgia Institute of Technology from Sept. 2017 to Sept. 2018 under the guidance of Prof. Zhuomin Zhang. Currently, Dr. Wu is an associate researcher at Shandong Institute of Advanced Technology. Dr. Wu's main research interest is on thermal

radiative properties of anisotropic materials and applications. He has published about 60 peer-reviewed journal papers and given three conference presentations. His Ph.D. thesis was published by Springer Nature and was recognized as outstanding doctoral research. Dr. Wu is the winner (along with his advisors) of the 2019 Hartnett-Irvine Award by the International Centre for Heat and Mass Transfer. In addition, his work about hyperbolic materials was selected as “Optics in 2020” by Optics & Photonics News. Besides, two of his papers are selected as cover papers by ES Energy & Environment.

Publisher’s Note: Engineered Science Publisher remains neutral with regard to jurisdictional claims in published maps and institutional affiliations.